

HIGH POWER MPD THRUSTER DEVELOPMENT AT THE NASA GLENN RESEARCH CENTER

Michael R. LaPointe

Ohio Aerospace Institute, 22800 Cedar Point Road, Cleveland, OH 44142
(216) 433-6192, michael.lapointe@grc.nasa.gov

Abstract. The NASA Glenn Research Center (GRC) is developing MW-class electromagnetic thrusters to meet a variety of future mission applications. This paper describes the pulsed, high power MPD thruster test facility at GRC, and provides preliminary voltage-current measurements obtained with a MW-class baseline thruster design. A flexure-based thrust stand is currently being modified to reduce magnetic tare forces encountered during high current thruster operation. Once the thrust stand is completed, the combined measurements of thrust, voltage, and current will be used to determine thruster efficiency for various high power MPD thruster designs. Through a combination of advanced numerical modeling and experimental validation, the near-term goal of the GRC test program is to design and demonstrate gas-fed MPD thrusters with efficiencies in excess of 50%.

INTRODUCTION

In its basic form, the magnetoplasmadynamic (MPD) thruster consists of a central cathode surrounded by a concentric anode (Fig. 1). A high-current arc is struck between the anode and cathode, which ionizes and accelerates a gas propellant. In self-field thrusters, an azimuthal magnetic field produced by the return current flowing through the cathode interacts with the radial discharge current density flowing through the plasma to produce an axial Lorentz body force, giving rise to the appellation of Lorentz Force Accelerator or LFA often encountered in the literature. In applied-field versions of the thruster, a solenoid magnet surrounding the anode provides additional radial and axial magnetic fields that can help stabilize and accelerate the plasma discharge.

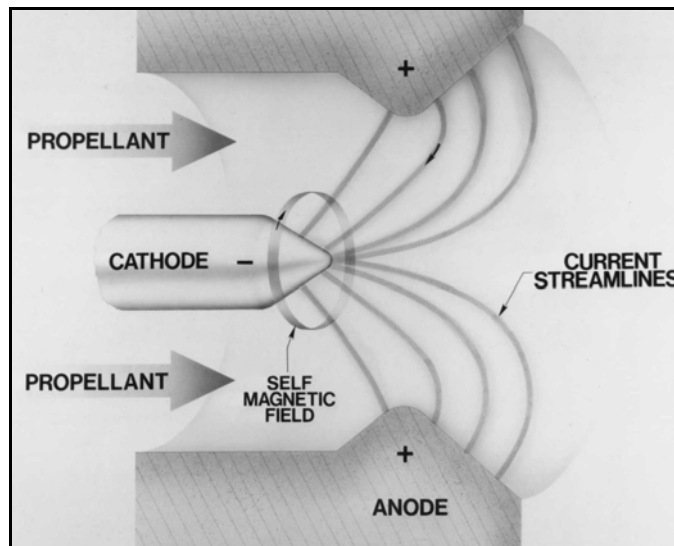


FIGURE 1. Self-field MPD thruster diagram

Initially developed in the 1960's, the MPD thruster has been funded intermittently over the past few decades, leading to slow but steady improvements in performance. For a detailed history of MPD thruster development, the reader is referred to a number of review papers that chronicle the progress and challenge of this promising high power propulsion technology (Nerheim, 1968; Sovey, 1988; Myers, 1991). Various thruster geometries

have been operated using a variety of propellants, with the most efficient performance to date achieved using lithium vapor propellant. Lithium-fed MPD thrusters developed by the Moscow Aviation Institute in Russia have reportedly demonstrated 45% efficiency at power levels approaching 150-kW, and lithium-fed devices are currently being investigated in the United States by the NASA Jet Propulsion Laboratory and Princeton University (Tikhonov, 1997; Kudysis 2001; Polk, 2000). A possible issue with lithium is that it is a condensable propellant, and has the potential to coat spacecraft surfaces and arrays. In addition, the maximum achievable specific impulse (Isp) with lithium is around 7500 s, while future power-rich robotic and piloted outer planet missions will require specific impulse values approaching 10000 s. These higher Isp values are achievable with hydrogen, hence non-condensable gas propellants are also being investigated to better understand and improve gas-fed thruster performance. Prior gas-fed thruster efficiencies have typically been lower than devices operated with lithium (Sovey, 1988; Myers, 1991; Choueiri, 1998), but recent numerical models indicate that significantly improved performance can be achieved through the use of modified electrode geometries and the proper application of expansion nozzles and/or applied magnetic fields (Mikellides, 2000a; Mikellides, 2000b; LaPointe 2002). The use of hydrogen and other non-condensable gas propellants mitigates possible ground handling and spacecraft contamination issues associated with the use of lithium, and may provide efficient thruster operation over a wide range of operating conditions. The NASA GRC effort has therefore focused on the development of gas-fed thruster technologies.

PULSED MPD THRUSTER TEST FACILITY

The high power plasma thruster test facility at the Glenn Research Center consists of a high-energy capacitor bank, pulse-forming network, vacuum chamber, and automated control systems. A flexure-based thrust stand for pulsed MPD thruster impulse measurements has been fabricated, and is currently undergoing modifications to reduce magnetic tare forces and make the stand more sensitive at low thrust values. A brief description of each of the major facility elements is provided below.

Capacitor Bank

The pulse-forming network used for quasi-steady MW-class thruster testing consists of 46 capacitors and 7 inductors arranged in a 7-element Guillemin network. Each capacitor is rated for 10-kVDC, with an expected shot life of 10^4 discharges at maximum charge voltage. The total bank capacitance is 4.88-mF, providing a maximum stored energy of 250-kJ at full charge. Switching is performed by a solid-state thyristor rated for 15-kV and 50-kA peak current, although the bank can also be fired using a back-up triggered spark-gap switch. Six of the inductors consist of insulated 3/8" copper tubing wound around short sections of 10.75" (27.3 cm) OD pvc pipe; the seventh inductor, which channels most of the discharge current, is constructed of insulated 2-AWG stranded cable. A 0.12- Ω matching resistor, rated for 10-kV and 250-kJ, is located in series between the switch and load. The discharge period is approximately 2×10^{-3} s, with less than 10% current ripple over the discharge plateau. Representative current and voltage traces obtained with a 0.013- Ω resistive load used to simulate an MPD thruster discharge are presented in Fig. 2.

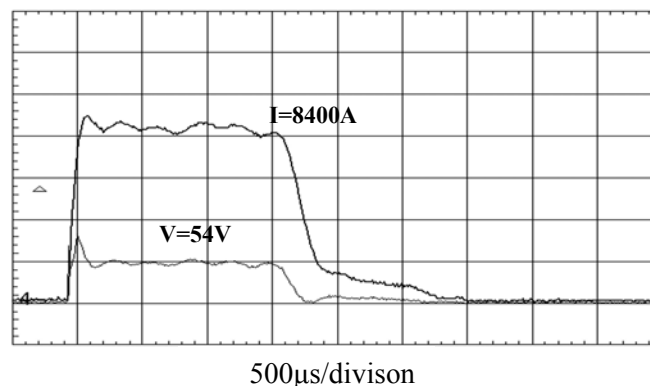


FIGURE 2. Representative voltage and current waveforms, 0.013- Ω resistive load

The capacitor bank and PFN are isolated from ground during each discharge. A 1000- Ω , 250-kJ resistor tied across the bank is used to discharge the capacitors in the event of a thruster malfunction or safety interlock violation. The physical dimensions of the capacitor bank are 4.5 m (15 ft) long by 2.1 m (7 ft) high by 0.9 m (3 ft) wide. A portion of the capacitor bank and PFN are shown in Fig. 3.

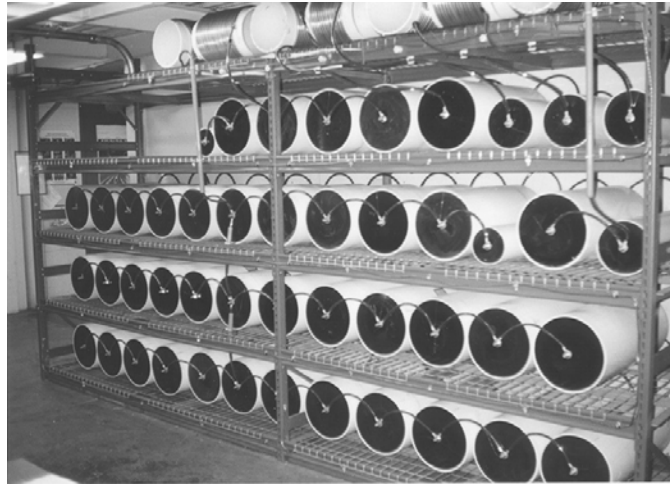


FIGURE 3. Portion of NASA GRC high power capacitor bank and PFN

Vacuum Chamber

Pulsed MPD thruster tests are conducted in NASA GRC Vacuum Facility 1 (VF1). The vacuum chamber, shown in Fig. 4, is 1.5-m (5 ft) in diameter by 4.5-m (15 ft) long. Access to the chamber interior is provided through an endcap mounted on a balanced swing-arm. The tank is pumped by two 0.8-m (32") diameter oil diffusion pumps and a mechanical roughing pump, and is capable of reaching an unloaded base pressure of 10^{-6} torr (8×10^{-9} Pa).

The vacuum tank is located on the floor above the capacitor bank, and power is cabled to the tank through high voltage feedthroughs located on a 1-m (36") bottom flange. Instrumentation and gas feedthroughs are located on a 0.4-m (16") side port, with additional access available through several 0.1-m (4") ports mounted to the facility endcap. A separate 0.4-m side port provides power cable access for a magnetic field coil, described in a later section of the paper.



FIGURE 4. NASA GRC Vacuum Facility 1 (VF-1)

Propellant Plenum

The propellant gas plenum is mounted to a test cart located beside VF1 (Fig 4). The cylindrical plenum chamber is constructed of stainless steel, with an interior volume of $2.5 \times 10^{-2} \text{ m}^3$ ($1.5 \times 10^3 \text{ in}^3$). Stainless steel tubing connects one end of the plenum to a regulated gas bottle, while the other end is connected to a pneumatic actuator powered by a fast acting solenoid valve. Gas flow from the actuator can be directed either to the thruster through a side flange located in VF-1, or to a small calibration chamber located on the test cart. The cylindrical calibration chamber, also constructed of stainless steel, has an internal volume of $6.1 \times 10^{-3} \text{ m}^3$ ($3.7 \times 10^2 \text{ in}^3$) and is used to measure the amount of gas discharged during pulsed plenum operation. Both the propellant plenum and the calibration chamber are outfitted with wide-ranging pressure gauges (dual pirani gauge and diaphragm manometer), capable of measuring pressure values from 10^{-3} torr to 1500 torr. During calibration, the propellant plenum pressure is set to a given value, and the calibration chamber is evacuated to vacuum. Gas from the propellant plenum is discharged into the calibration plenum, and the resulting pressure rise is recorded. Knowing the pressure change and the chamber volume allows the propellant mass injected into the calibration chamber to be calculated, and dividing this mass by the total response period of the pneumatic actuator provides the propellant flow rate for the pulsed discharge. The flow period of the actuator can be set between 60-ms and 230-ms through the use of a variable resistor in the control circuit; the latter value has been used to reduce the effect of uncertainty in the actuator opening and closing response times. The calibrated mass flow rates are estimated to have uncertainties of $\pm 5\%$.

Applied-Field Magnet

Prior research has shown that it may be advantageous to operate MPD thrusters with axial and radial magnetic fields provided by a solenoid magnet surrounding the anode (Sovey, 1988; Myers, 1991; Mikellides, 2000a; Mikellides, 2000b). To provide this capability, 4-AWG insulated cabling was wound on a 0.2-m (8") OD pvc pipe to form a solenoid test magnet. The magnet consists of 7 layers with 18 turns per layer. The magnet cabling is un-cooled, limiting both the maximum current and period of operation, but the simplicity of operation and the attainable field strength over the required thruster pulse period outweigh these disadvantages. Power is supplied by a 50-kW constant-current arc welder, capable of delivering up to 1000 A to the magnet. The measured axial magnetic field strength at the center of coil is roughly $5 \times 10^{-4} \text{ T/A}$, while at the end of the coil the axial field along the centerline is approximately $3.3 \times 10^{-4} \text{ T/A}$.

Control System

The events leading up to a pulsed thruster discharge are controlled by an automated sequencing system mounted in the MPD control rack. If the applied-field magnet is to be used, the magnet power supply is preset to the desired current level. The capacitor bank is then charged to the desired voltage using a 4-kW, 10-kV power supply located in the control rack. Once the bank is charged to the desired voltage, the charging supply is disengaged and the test sequence is initiated. For applied-field operation, the magnet power is turned on for a period of 4.5 s, sufficient to establish a constant field distribution within the thruster and allow residual thrust stand disturbances due to switching on the magnet to damp away. Toward the end of this period, the propellant plenum solenoid is activated to provide a gas pulse to the thruster; as noted, the duration of the gas pulse can be set from 60-ms to 230-ms, with the present value set at 230-ms to reduce uncertainties in the pulsed propellant mass flow rate. The capacitor bank switch is triggered toward the end of the gas flow period, providing an approximately 2-ms, high current discharge to the thruster. Once the bank has fired, the control sequence turns off the gas flow and magnet current, and the logic system is then reset to initiate another test sequence.

Thrust Stand

The thrust stand currently being developed for high power MPD thruster testing is based on a simple flexure design (Fig 5). The thruster is mounted to a stiff horizontal plate, which in turn is supported by four thin, contoured aluminum flexures mounted to a bottom support plate. Current is fed to the thruster through high voltage coaxial cables, with return currents traveling through the cable shields to reduce magnetic tare forces on

the thrust stand. During discharge, the upper plate of the thrust stand is horizontally displaced by the thruster impulse. To measure the resulting impulse, a calibrated load cell, mounted on a sturdy support bracket bolted to the bottom plate of the thrust stand, is placed in firm contact with the moveable upper plate of the thrust stand. Movement of the upper plate is restricted by contact with the load cell, and an oscilloscope measures the voltage response of the load cell produced by the thruster impulse. The thrust stand is calibrated prior to testing using an electronic impact hammer; the hammer tip impacts a separate load cell mounted on a cross bar across the face of the thruster anode, and the resulting impulse is measured by the load cell on the thrust stand. The thrust stand configuration does not allow in-situ calibration under vacuum conditions; however, a solid-state inclinometer mounted beneath the top plate of the thrust stand is used to provide information on the initial and final orientation (tilt) of the stand. No significant differences have been observed between thrust stand orientations at rest in air or under vacuum, providing some assurance that the measured impulse values will closely correspond to the calibrated thrust stand values. Nevertheless, the angular orientation of the stand before and after each shot is recorded to allow refined calculations of the delivered impulse, if required. Tare force measurements for the thrust stand are currently being obtained, and will be reported in a future publication.

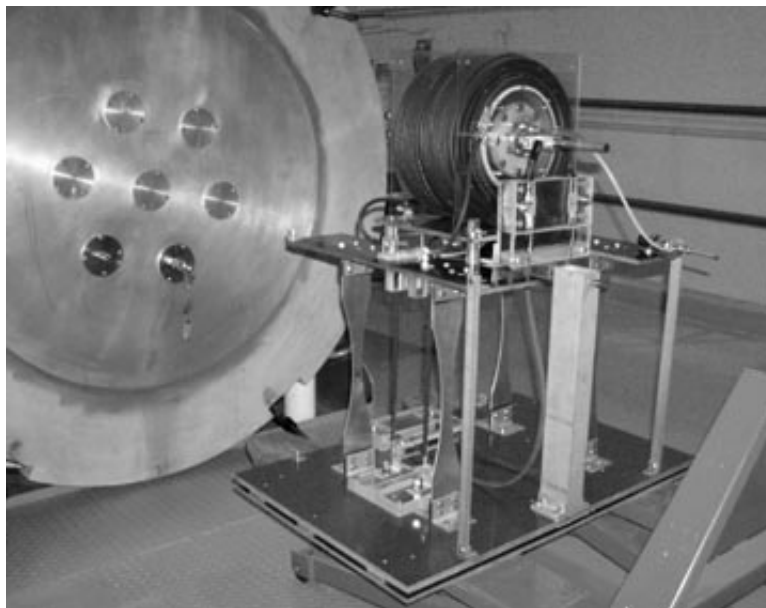


FIGURE 5. MPD thruster mounted on flexure-based thrust stand

Data Collection

The primary diagnostics at this stage of facility development include thruster voltage and current, thrust stand displacement, and magnet coil temperature. Thruster voltage and current are used to calculate the thruster power. Voltage, current, thrust, and mass flow rate are combined to determine thruster efficiency, η :

$$\eta = \frac{T^2}{2\dot{m}VJ} \quad (1)$$

where T is the thrust (N), \dot{m} is the propellant mass flow rate (kg/s), V is the discharge voltage, and J is the thruster operating current.

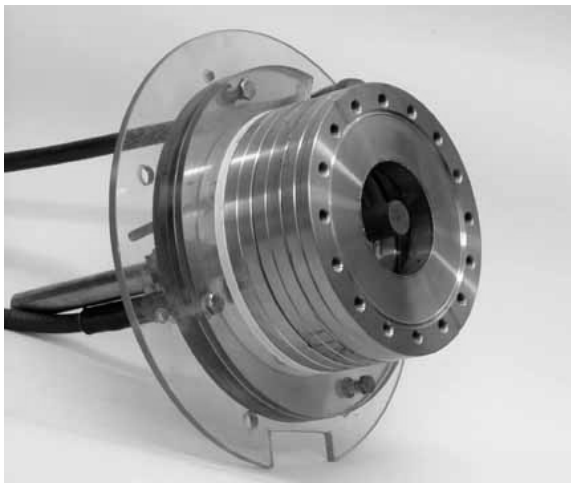
Digital oscilloscopes measure and record the thruster voltage, thruster current, and load cell voltage waveforms, which are then transferred to a desktop computer for later analysis. Differential voltages are measured across the thruster electrodes using a voltage attenuation (resistor network) circuit to scale the voltage channels and prevent waveform clipping by the oscilloscopes. The differential voltage is measured over a 500- μ s period in a quiescent

portion of the 2-ms discharge, with a typical error of $\pm 5\%$. Two independent current monitors (transformers) are used to record the pulsed current into and out of the thruster. The coils are rated for 50-kA peak current, a current-time product of 65 A-s, and a rise time of 2.5×10^{-7} s. The discharge current is measured over the same 500- μ s period as the differential voltage; due to slight rippling in the current waveform, the measurement error is typically within $\pm 10\%$. Because the thrust stand is currently undergoing tare tests, error bars for thrust measurements made by the load cell are not yet reportable.

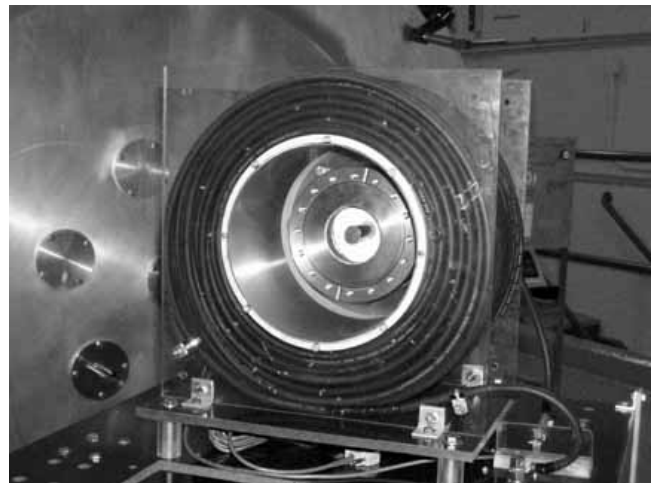
The temperature of the thruster is not expected to increase significantly during each 2-ms discharge, and the period between pulses is sufficiently long (\sim minutes) that thruster electrode temperature measurements are not required. However, the magnet coil current will resistively heat the magnet during the few seconds of operation required for applied-field MPD thruster tests, hence thermocouples have been embedded in the coil to monitor the temperature rise and to signal when testing should be suspended to cool the magnet. Although no plasma diagnostics are currently in place, plans call for the installation of Hall and Langmuir probes to provide density and temperature measurements in the thrust chamber and plume region.

BASELINE MPD THRUSTER

Preliminary facility operation was evaluated using the baseline laboratory model thruster shown in Figures 6a and 6b. Similar in geometry to the Princeton University benchmark MPD thruster (Choueiri, 1998), the baseline thruster anode is constructed of stainless steel disks bolted together to form an anode chamber and constricted lip region. The chamber depth is approximately 3.2 cm from backplate to anode face, with an internal chamber radius of 5 cm. The anode lip is 2 cm wide with a 2 cm internal radius. A 0.95-cm radius tungsten rod cathode extends approximately 8-cm from the backplate. The electrically insulating backplate separating the anode and cathode is composed of combat-grade boron nitride. An annular tube with a bend radius of 4-cm fits within a circular groove in the boron nitride; propellant enters the thruster through 10 evenly spaced 1/16" (0.15 cm) diameter holes drilled in the outer face of the annular tube. The thruster assembly is secured within the solenoid magnet with fitted lexan support disks, and the whole assembly is mounted to the top plate of the thrust stand.



(a)



(b)

FIGURE 6. (a) Baseline lab-model MPD thruster; (b) baseline thruster mounted within solenoid magnet

The thrust stand was not fully calibrated in time for this paper, allowing only preliminary thruster voltage and current data to be measured and reported below. The baseline MPD thruster was operated at propellant plenum pressures corresponding to argon mass flow rates of 0.5-g/s (5×10^{-4} kg/s) and 1-g/s (10^{-3} kg/s). Preliminary voltage-current traces recorded for these mass flow rates are presented in Fig. 7.

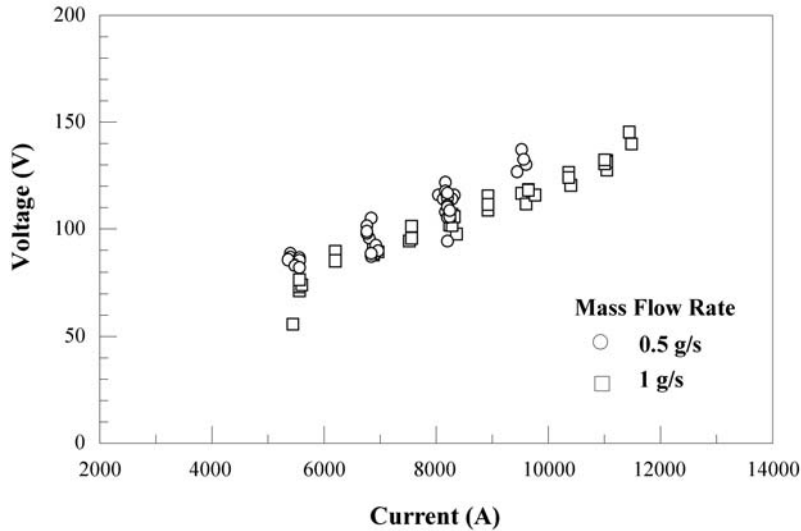


FIGURE 7. Preliminary baseline MPD thruster voltage-current data

The terminal thruster voltage obtained at a given discharge current is slightly lower at higher mass flow rates, consistent with prior benchmark thruster data (Gilland, 1987; Choueiri, 1998). The nearly linear voltage-current characteristics and only slight dependence on mass flow rate displayed by the data in Figure 7 does not show the characteristic J^3 dependence associated with the electromagnetic acceleration of a fully ionized propellant. In addition, the voltage traces recorded for each shot were fairly flat and did not display the signal hash typically associated with the onset of thruster instabilities; representative thruster voltage and current traces are shown in Fig. 8. It thus appears that the baseline thruster was operating at less than full propellant ionization and below the onset of plasma instabilities for the range of currents shown in Fig. 7. The maximum thruster power corresponding to the data in Fig. 7 was approximately 1.3-MW for an argon mass flow rate of 0.5-g/s, and 1.7-MW for an argon mass flow rate of 1-g/s. The thruster apparently operates stably at these power levels, which bodes well for thruster testing at higher power levels. Continued high power testing awaits the completion and commission of the thrust stand assembly, which will provide measurements of the baseline thruster impulse and allow the calculation of thruster efficiencies.

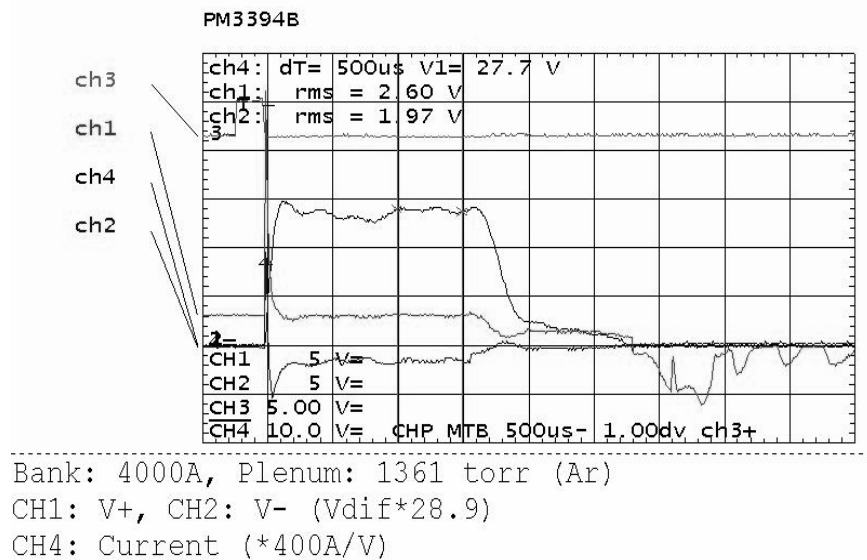


FIGURE 8. Representative voltage and current traces for baseline MPD thruster operated at 1.3-MW

MPD THRUSTER MODELING

With funding provided by the NASA Glenn Research Center, the Arizona State University is modifying and using the state of the art MACH2 code to simulate high power MPD thruster performance. Originally developed in the 1980s by the Mission Research Corporation to simulate collisional plasma problems, MACH2 is a time-dependent, two-dimensional, axisymmetric, multi-material, code whose multi-block structure makes it suitable for solving problems with complex geometries [Mikellides 2000a]. The computational mesh can move in an Arbitrary Lagrangian-Eulerian (ALE) fashion, allowing the code to be used for both diffusive- and dispersive-dominated problems. The mesh can be refined using a variety of adaptive schemes to capture regions of varying characteristic scale. The set of single-fluid MHD equations is time advanced with finite-volume spatial differencing, and the boundary conditions are applied via a ghost-cell technique such that no special conditional statement is necessary at the boundaries.

The mass continuity and momentum equations assume a compressible viscous fluid, with the latter including both real and artificial viscosity effects. The stress-deviator can be chosen to evolve under elastic stress for strength of material calculations or modeled as a Newtonian fluid to upgrade the code to a Navier-Stokes solver. The code includes two ablation models that allow mass addition due to solid evaporation, which have been successfully employed to model ablation-fed pulsed plasma thrusters. The electrons, ions and radiation field are in thermal non-equilibrium, so MACH2 solves three energy equations. These include thermal conduction with anisotropic transport and three different models for radiation cooling. Evolution of the magnetic field is prescribed by the induction equation that includes resistive diffusion, the Hall effect and the thermal source for magnetic fields. Various models for the plasma resistivity are available, consisting of classical anisotropic resistivity, several anomalous resistivity models, and contributions from electron-neutral collisions applicable to weakly ionized gases. In many engineering applications, the sources of magnetic flux are the applied currents produced from externally applied voltage differentials. To model this, the code includes a variety of circuit simulations such as LRC, Pulse-Forming-Networks, sine-waveforms, and several others.

The set of the MHD equations is completed by an equation of state that can be either analytic or tabular. The latter is provided by the SESAME library, which includes semi-empirical models for the thermodynamic properties, transport coefficients, (including opacities) and average ionization state under local thermodynamic equilibrium. These models have been constructed and are being maintained by the T-1 and T-4 groups at the Los Alamos National Laboratory. The level of sophistication and capability provided by the MACH2 code has been instrumental in providing invaluable insights for a variety of plasma problems, and its diverse success has established the code as the primary numerical tool in the design of MW-class MPD thrusters at NASA GRC. Recent simulations using MACH2 for MPD thruster simulations include an analysis of the Japanese MY-II MW-class self-field thruster, which accurately predicts thrust and current streamline distributions, and a new nozzle-anode MPD thruster designed to improve self-field thruster efficiency by recovering a fraction of the radial thrust and thermal power losses [LaPointe 2002]. The nozzle anode thruster has been fabricated (Fig 9), and will be tested in NASA GRC VF-1 during FY03.

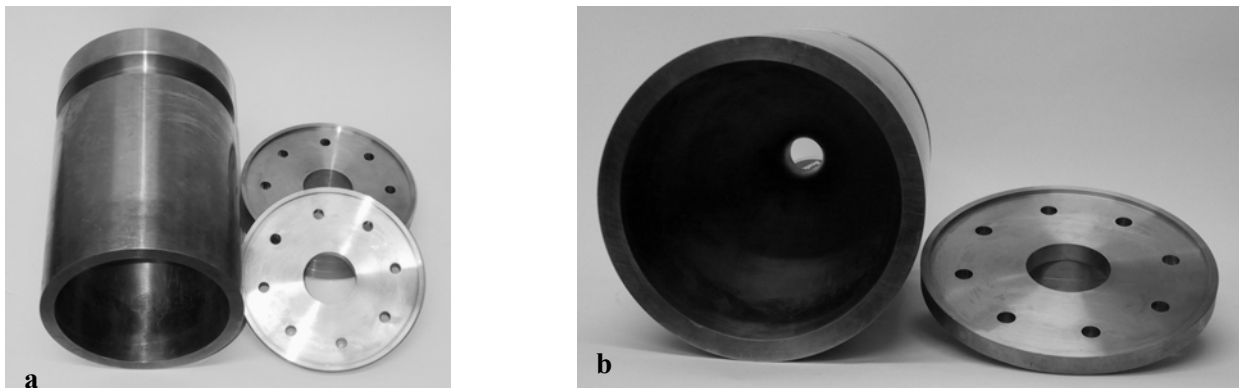


FIGURE 9. Nozzle MPD thruster anode (a) side view, (b) front view.

CONCLUDING REMARKS

Within the next few months, the baseline MPD thruster will be tested with argon and hydrogen propellants in both self-field and applied-field modes of operation at power levels from 500-kW to 5-MW. Voltage and thrust measurements will be obtained for a wide range of discharge currents and propellant mass flow rates, providing efficiency calculations and allowing thruster performance to be fully characterized. Concurrent with the experimental effort, the state of the art magnetohydrodynamics code, MACH2, will be used at Arizona State University to model the performance of various self-field and applied-field MPD thruster geometries to gain deeper insight into gas-fed thruster physics and improve the performance of these devices. Efforts will also be initiated in FY03 at Kettering University to develop an electrode sheath voltage model for future incorporation into the MACH2 code.

The experience gained in operating the baseline and nozzle MPD thrusters, coupled with the improved understanding provided by the corresponding MACH2 simulations, is expected to lead to the development of more efficient self-field and applied-field MPD thrusters. During 2003, the MACH2 code will be used to design new high power thrusters capable of achieving at least 50% efficiency with specific impulse values of around 5000-s. These designs will be fabricated for quasi-steady operation, and tested in the pulsed high power facility at NASA GRC. The main goal of this combined numerical and experimental effort will be the demonstration of more efficient MPD thruster operation; the issue of improved thruster lifetime will necessarily wait for steady-state high power thruster operation.

ACKNOWLEDGMENTS

This research is funded through a cooperative agreement between the Ohio Aerospace Institute and the NASA Glenn Research Center, whose support is gratefully acknowledged. The author also acknowledges the invaluable technical assistance of Mr. Gene Strzempkoski, NASA GRC, lead electronics engineer for the MPD project; Mr. Joseph Dick and Mr. George Rodriguez, Akima Corporation, for the initial construction and continued electrical support of the capacitor bank and PFN; and Mr. James Coy and Ms. Donna Neville, NASA GRC, for assistance with mechanical designs and operation of the VF-1 vacuum facility.

REFERENCES

- Choueiri, E. and Zeimer, J., "Quasi-Steady Magnetoplasmadynamic Thruster Measured Performance Database," AIAA-98-3472, 34th Joint Propulsion Conference, Cleveland, OH, July 1998.
- Gilland, J. H. Kelly, A. J., and Jahn, R. G., "MPD Thruster Scaling," AIAA Paper 87-097, 19th International Electric Propulsion Conference, Colorado Springs, CO, May 1987.
- Kudysis, A., Emsellem, G., Cassady, L., Polk, J., and Choueiri, E., "Lithium Mass Flow Control for High Power Lorentz Force Accelerators," in *Space Technology and Applications International Forum (STAIF) 2001*, edited by M. El-Genk, AIP Conference Proceedings 552, Melville, New York, 2001, pp. 908-915.
- LaPointe, M. R. and Mikellides, G., "Design and Operation of MW-Class MPD Thrusters at the NASA Glenn Research Center", AIAA-2002-4133, 38th AIAA Joint Propulsion Conference, Indianapolis, IN, July 2002.
- Mikellides, P. G., Turchi, P. J., and Roderick, N. F., "Applied-Field Magnetoplasmadynamic Thrusters, Part 1: Numerical Simulations Using the MACH2 Code" *J. Propulsion and Power*, **16** (5), 887-893 (2000a).
- Mikellides, P., and Turchi, P., "Applied-Field Magnetoplasmadynamic Thrusters, Part 2: Analytic Expressions for Thrust and Voltage" *J. Propulsion and Power*, **16** (5), 894-901 (2000b).

- Myers, R., Mantenieks, M., and LaPointe, M., "MPD Thruster Technology," NASA TM-105242, 1991.
- Nerheim, N. and Kelly, A., "A Critical Review of the Magnetoplasmadynamic Thruster for Space Applications," NASA CR-92139, Feb 1968.
- Polk, J., Tikhonov, V., Semenikhin, S., and Kim, V., "Cathode Temperature Reduction by Addition of Barium in High Power Lithium Plasma Thrusters," in *Space Technology and Applications International Forum (STAIF) 2000*, edited by M. El-Genk, Polk, AIP Conference Proceedings 504, Melville, New York, 2000, pp. 1556-1563.
- Sovey, J. and Mantenieks, M., "Performance and Lifetime Assessment of Magnetoplasmadynamic Arc Thruster Technology," NASA TM-101293, 1988.
- Tikhonov, V., Semenikhin, S., Brophy, J., and Polk, J., "Performance of 130-kW MPD Thruster with an External Applied Field and Lithium as Propellant," IEPC-97-120, 25th International Electric Propulsion Conference, Cleveland, OH, 1997.